

Experimental study of flexural behaviour of GFRP reinforced concrete beams

C. Barris, Ll. Torres, A. Turon, M. Baena & C. Miàs
University of Girona, Girona, Spain

ABSTRACT: Concrete members reinforced with fibre-reinforced polymers (FRP) exhibit large deflections and crack widths compared with steel reinforced concrete members, due to the low modulus of elasticity of FRP. This study presents the results and discussion of experimental tests under four-point bending load for 24 Glass-FRP (GFRP) reinforced concrete beams. The main purpose of the study is the evaluation of short-term serviceability behaviour. The effects of the strength of concrete, the reinforcement ratio and the effective depth on deflection are investigated.

1 INTRODUCTION

Corrosion in steel as a structural reinforcement in aggressive environments can cause important damages in RC structures. In order to avoid these pathologies, the use of fiber reinforced polymer (FRP) rebars as a longitudinal reinforcement is suggested. Due to its lower modulus of elasticity compared with steel, larger deflections and crack widths are expected, and therefore, the design of these elements is often governed by the limit state of serviceability.

In the last years, several codes of practice have provided formulation for the short-term deflection prediction. ACI 440 (2006) and ISIS Canada (2001) suggest a modification in Branson's formula in order to consider the lower modulus of elasticity of FRP rebars and include a bond coefficient that depends on the rebar type. CAN/CSA-S806 (2002) approach is based in curvature integration along the beam, assuming a tri-linear moment-curvature relation, neglecting the tension-stiffening effect. Several tests (Benmokrane et al, 1996, Al-Sunna, 2006) show that deflections tend to exceed the deflection due to linear cracked moment of inertia at a relatively low load level.

The preliminary results of an experimental programme of 24 beams tested under 4 point load are presented. The main purpose of the study is the evaluation of short-term serviceability behaviour. The beams are tested under static load to investigate the effects of the strength of concrete, the reinforcement ratio and the effective depth on cracking and deflection.

2 EXPERIMENTAL PROGRAMME

2.1 Beams Specifications

The experimental programme consisted in two series of six GFRP RC beams. For each series, two specimens were tested (types *a* and *b*) giving a total amount of 24 beams. The beams were *B* mm wide, 190 mm high and 2100 mm long, and were tested under a four-point bending load. The distance between supports was 1800 mm, and the shear span 600 mm, so the distance between loads was 600 mm (Fig.1). The shearspan was reinforced with steel stirrups

($\phi 8\text{mm}/70\text{mm}$) in order to avoid shear failure and minimize shear effects. In the pure bending zone no stirrups were provided. As a top reinforcement, $2\phi 6$ steel rebars were used to hold stirrups in the shear span zone.

For each beam series, the effect of the reinforcement ratio and the effective depth/height relation were studied by using three different amounts of longitudinal reinforcement and two different covers. For every amount of reinforcement, the width of the beam was changed according to these parameters. In each series a different strength of concrete was used. Specimen type *a* was initially uncracked and specimen type *b* had a pre-crack in the midspan section to ensure the creation of a crack in a known specific position.

The geometric and reinforcement details of the beams are shown in Figure 1 and Table 1.

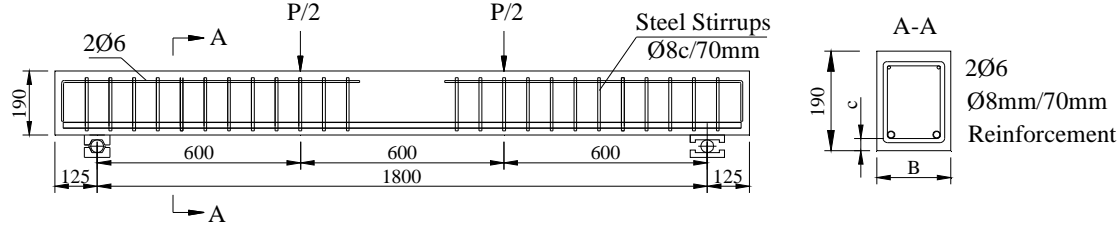


Figure 1. Geometric and reinforcement details

Table 1. Geometric characteristics of sections and properties of concrete

Beam Designation	<i>B</i> (mm)	<i>c</i> (mm)	<i>d/h</i>	Main Rebar	Reinforcement ratio, ρ (%)	Compressive Strength, f_c (MPa)
C1-212-D1	140	20	0.86	$2\phi 12$	0.99	32.1
C1-216-D1	140	20	0.85	$2\phi 16$	0.99	32.1
C1-316-D1	140	20	0.85	$3\phi 16$	1.77	32.1
C1-212-D2	160	40	0.75	$2\phi 12$	1.77	32.1
C1-216-D2	160	40	0.74	$2\phi 16$	2.66	32.1
C1-316-D2	160	40	0.74	$3\phi 16$	2.66	32.1
C2-212-D1	140	20	0.86	$2\phi 12$	0.99	45.0
C2-216-D1	140	20	0.85	$2\phi 16$	0.99	45.0
C2-316-D1	140	20	0.85	$3\phi 16$	1.77	45.0
C2-212-D2	160	40	0.75	$2\phi 12$	1.77	35.3
C2-216-D2	160	40	0.74	$2\phi 16$	2.66	45.0
C2-316-D2	160	40	0.74	$3\phi 16$	2.66	45.0

2.2 Materials

Two types of concrete strength were used for both series of beams. Concrete C1 stands for a 25 MPa concrete compressive strength and C2 for a 45 MPa compressive strength (Table 1). E-CR GFRP ComBAR (Schöck) rebars were used as a flexural reinforcement. The mechanical properties of these rebars were obtained by a uni-axial tension test and are shown in Table 2.

Table 2. Mechanical properties of GFRP Rebar

Diameter (mm)	Rupture Tensile Strength, f_{tu} (MPa)	Modulus of Elasticity, <i>E</i> (MPa)
12	1353	63252
16	995	64152

2.3 Experimental Setup and Instrumentation

Each beam was simply supported. A hydraulic jack transmitted the load to the test beam by a spreader beam. The load was applied in displacement control mode, and all data was collected by a data acquisition system. Every 10 kN of applied load, the load applicator was paused to control cracks and strains and to take notes.

In beams type C1, horizontal (top and bottom) and vertical strain was measured by means of a mechanical extensometer over a gauge length of 150 mm along the beam. Therefore, a mean curvature was obtained for every load step. In beams type C2, the mechanical extensometer was only implemented in the pure bending zone. In order to control the deflection of the tested beam, five transducers (LVDT and strain gauge based transducers) were used: one at each support, one in the midspan section and two at 450 mm distance from the supports.

All beams were instrumented with two inclinometers, each one at 225 mm from the midspan section, so the difference of angles and the average curvature of the pure bending zone were controlled. In beams type *b*, the midspan section was instrumented with three concrete strain gauges at the surface of the beam (one on the top surface, one at 20 mm of the top and one at 48 mm of the top) to control the evolution of the concrete strain with load. An additional horizontal transducer was used in the midspan section of these beams at the height of the longitudinal reinforcement to control the width of the midspan crack. Some of the *b* beams were internally instrumented with strain gauges on the GFRP rebar. These gauges were distributed over the shearspan length and concentrated in the midspan zone. Figure 2 shows the test setup and the instrumentation.

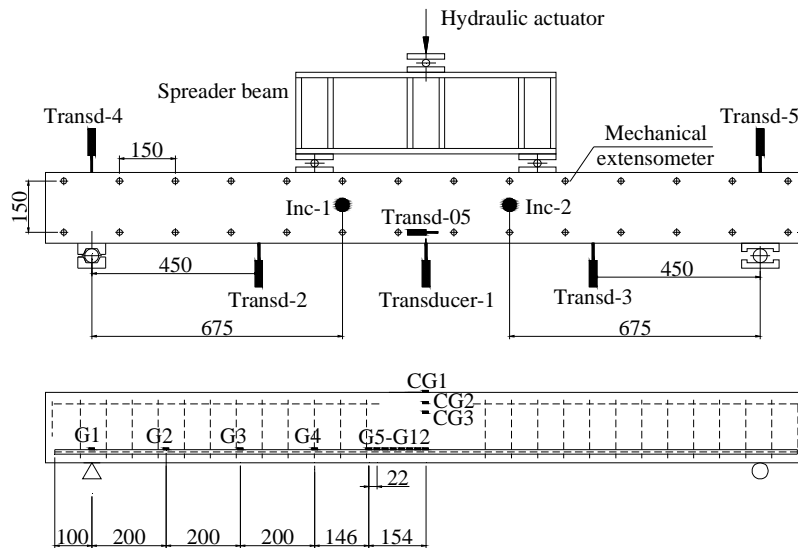


Figure 2. Test setup

3 TEST RESULTS AND DATA ANALYSIS

3.1 Load – Rebar strain along the beam

Figure 3a shows a typical experimental Load – Rebar Strain relation. In the midspan section, gauges G6 and G10-G11 reach the maximum values of strain, which is explained by the formation of cracks near these positions (Fig. 3b), meanwhile in the shearspan, gauge G1 (located over the support) has almost a negligible strain, and gauges G2 to G4 increase their value in a non-linear path.

3.2 Load – Concrete strain in midspan section

A typical representation of Load – Concrete Strain relation is shown in Figure 4. It is observed that before cracking, top concrete strain is almost negligible, but when cracking occurs, its value increases considerably. The maximum concrete strain in compression is reached by the top surface strain, whereas the gauge located at 48 mm from top can be either in compression or in

tension, depending on the position of the neutral axis. The experimental strain at top surface is compared with the theoretical approach obtained by cracked-section analysis (CSA). As shown in Figures 4a, b, cracked-section analysis underestimates the strain at midspan section. This difference can be explained because of the assumptions considered in the cracked-section analysis.

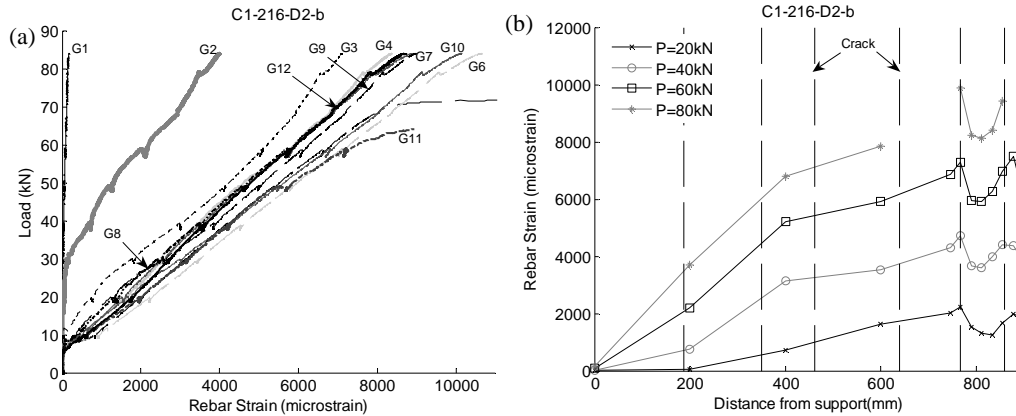


Figure 3. (a) Rebar strain vs. Load (b) Rebar strain along the length of the beam

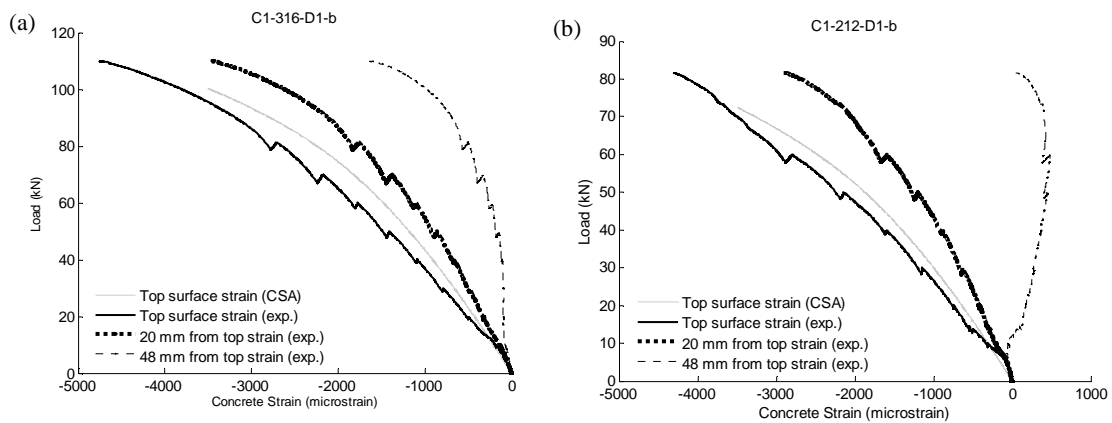


Figure 4. Load – Concrete Strain (a) Beam C1-212-D1-b, (b) Beam C1-316-D1-b

3.3 Moment – Curvature in midspan section

Figure 5 shows the experimental Moment – Curvature relation deduced from the inclinometers and the strain gauges at midspan section, and it is compared with the theoretically deduced from the Eurocode 2 (CEN 2004) approach. It can be observed that both data (deduced from inclinometers and from strain gauges) fit reasonably well Eurocode 2 approach.

3.4 Neutral axis depth in midspan section

An experimental position of neutral axis is calculated from the measured values of the concrete and FRP strains. As it can be observed in Figure 6, the neutral axis depth decreases just after cracking occurs. Then, its value remains constant or slightly decreases, and it finally increases until the maximum load is achieved. The neutral axis depth is higher as reinforcement ratio increases, as it is expected to theoretically occur.

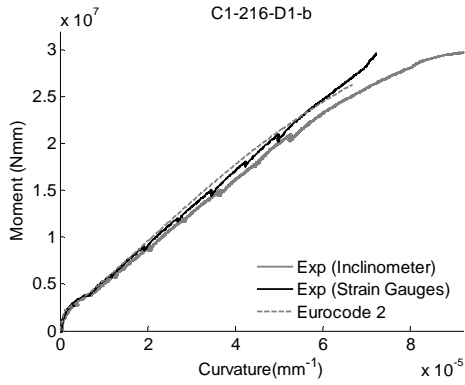


Figure 5. Moment – Curvature

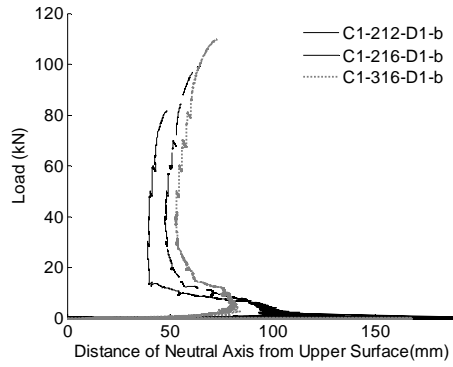


Figure 6. Neutral axis depth

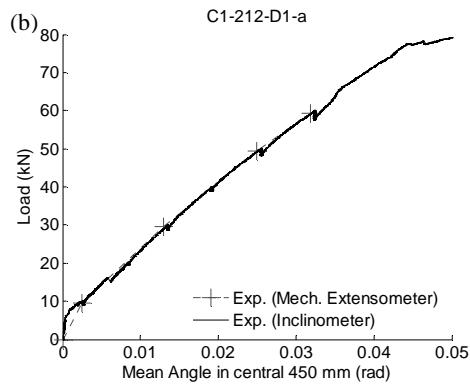
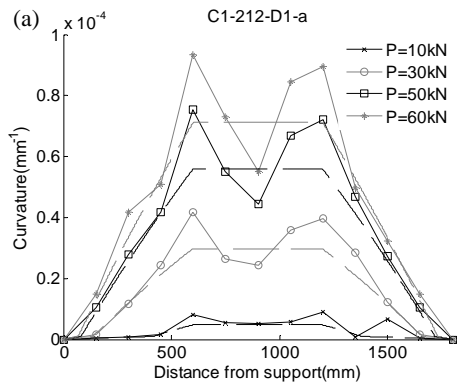


Figure 7. (a) Curvature distribution along the beam, (b) Mean angle in 450 central millimeters

3.5 Load – Deflection

An experimental Load – Deflection relation derived from the measurement of midspan transducer (taking into account the supports' displacement) is shown in Figure 8. This tendency is compared with theoretical approaches according to Eurocode 2 and ACI 440.1R-06.

The good repeatability in deflection behaviour between both specimens of the same beam can be observed from Figure 8. Up to a service load, both Eurocode 2 and ACI 440.1R-06 approaches compare reasonably well with the experimental tendency. However, for higher loads, both theoretical approaches underestimate the experimental value.

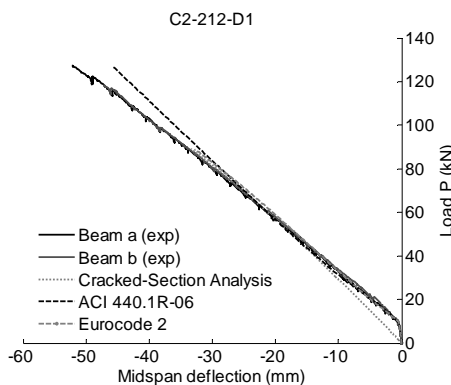


Figure 8. Load – Deflection

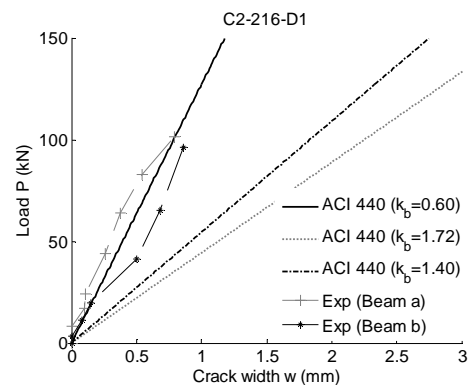


Figure 9. Load – Crack width

3.6 Cracking behaviour

The experimental crack width measured in the tension face of the beam is shown and compared with the predicted by ACI 440.1R-06 in Figure 9. Following ACI provisions, the crack width depends on a bond coefficient (k_b), which can vary from 0.60 to 1.72, and a design value of 1.40 can be assumed if bond is not known. As observed, the experimental crack width fits well with the minimum crack width predicted by ACI 440.1R-06, which proves the good bond between concrete and the bars used in the experimental programme.

4 CONCLUSIONS

The present paper shows the preliminary results of an experimental programme focused in study the serviceability behaviour of beams reinforced with GFRP rebars. 24 beams have been tested and analyzed under a four point bending test. The following conclusions have been obtained.

- A good repeatability in deflection behaviour for each couple of identical beams is observed (beams *a* and *b*).
- Gauges placed on FRP rebars show maximum values when a crack is created nearby them. Gauges placed on concrete show the evolution of concrete strain with load and allow obtaining an average neutral axis depth.
- The experimental moment-curvature relation fits reasonably well Eurocode 2 approach
- The neutral axis depth decreases just after cracking occurs. Then, its value remains constant or slightly decreases, and it finally increases until rupture.
- Although the curvature does not remain constant in the pure moment zone, the rotation in the central 450 mm can be evaluated by both the inclinometers and the average curvature derived from mechanical extensometer.
- For service load, flexural deflection behaviour approach of ACI 440.1R-06 and Eurocode 2 follow nearly well the experimental behaviour observed. However, after this value is reached, both theoretical approaches underestimate the experimental value.
- The observed crack width fits well with the predicted by ACI 440.1R-06 using a bond coefficient of 0.60.

5 ACKNOWLEDGEMENTS

The authors acknowledge the support provided by the Spanish Government (Ministerio de Educación y Ciencia), Project ref. BIA-2004-0523 and also the support of Schök Bauteile GmbH for the GFRP rebars supply.

6 REFERENCES

- ACI Committee 440 2006. Guide for the Design and Construction of Concrete Reinforced with FRP Bars (ACI 440.1R-06). *American Concrete Institute*, 2003, Farmington Hills, Mich, 45 pp.
- Al-Sunna, R., Pilakoutas, K., Waldron, P., Guadagnini, M. 2006. Deflection of GFRP Reinforced Concrete Beams. *Proceedings of the 2nd FIB Congress*, Napples, Italy, 5-8 June, 2006.
- Benmokrane, B., Chaallal, O. and Masmoudi, R. 1996. Flexural Response of Concrete Beams Reinforced with FRP Reinforcing Bars, *ACI Structural Journal*, 1996:93(1): 46-55.
- CSA 2002. Design and Construction of Building Components with Fibre-Reinforced Polymers (CAN/CSA-S806-02). *Canadian Standards Association*, Mississauga, Ontario, Canada. 177 pp.
- CEN 2004. Eurocode 2: Design of Concrete Structures – Part 1-1: General rules and rules for buildings (EN 1992-1-1:2004). *Comite Europeen de Normalisation*, Brussels, 225 pp.
- ISIS Canada 2001. Reinforcing Concrete Structures with Fibre Reinforced Polymers-Design Manual No. 3. *ISIS Canada Corporation*, University of Manitoba, Manitoba, Canada.